Journal of Electroanalytical Chemistry 847 (2019) 113197

Contents lists available at ScienceDirect

Journal of Electroanalytical Chemistry

journal homepage: www.elsevier.com/locate/jelechem

Enhanced electrochemical performance and thermal properties of Ni-rich $LiNi_{0.8}Co_{0.1}Mn_{0.1}O_2$ cathode material via CaF_2 coating

Shican Dai, Guanjie Yan, Long Wang, Liming Luo, Yaping Li, Yuting Yang, Hanhui Liu, Yue Liu, Mingliang Yuan*

Key Laboratory for Mineral Materials and Application of Hunan Province, School of Mineral Processing and Bioengineering, Central South University, Changsha, 410083, China

ARTICLE INFO

Keywords:
Lithium ion batteries
Li-rich cathode materials
CaF_2 coating
Storage deterioration
Elevated temperature

ABSTRACT

$LiNi_{0.8}Co_{0.1}Mn_{0.1}O_2$ (NCM811) is demonstrated as potential cathode material for next-generation lithium-ion batteries. However, the electrochemical performance of this material is severely inhibited by structural degradation and capacity decay, especially at elevated temperatures. Herein, we try to design an ultra-thin CaF_2 coating on the surface of NCM811 and examine the electrochemical performance. Physicochemical characterization results show that a CaF_2 layer with a thickness of 5–12 nm was successfully attached to the surface of microspheres, without significant changes in structure or morphology. Electrochemical tests indicate that calcium fluoride modified samples especially 3 wt% exhibit a surprising cycle capability and rate performance. What's more, Calcium fluoride coating can also improve the high temperature stability of cathode material, sample with 3 wt% CaF_2-coated shows an initial discharge specific capacity of 149.6 $mAhg^{-1}$ and a capacity loss of 20.32% after 50 cycles at 55 °C, whereas the pristine material is 150.4 $mAhg^{-1}$ and a severely capacity loss of 40.68%. The cyclic voltammograms (CV) and electrochemical impedance spectra (EIS) tests show that coated samples deliver a smaller potential difference (ΔV) and impedance after cycles, further confirming that CaF_2 coating can enhance the electrochemical performance of NCM811 material.

1. Introduction

Lithium-ion batteries (LIBs) are applied more and more widely in the field of energy storage system (ESS) and hybrid electric vehicles (HEVs) over the past decades. Among the main components of lithium battery, the anode material has been highly developed. What impedes further development of lithium ion battery is cathode material with low lithium storage capacity [1–3]. Therefore, it is of great significance to develop high performance cathode materials. Layered $LiNi_xCo_yMn_{1-x-y}O_2$ ($x > 0.5$) cathode with high energy density and acceptable price is one of the most promising materials for next generation of lithium-ion batteries, especially $LiNi_{0.8}Co_{0.1}Mn_{0.1}O_2$ (NCM811) [4,5]. However, the practical applications of this material at high voltages and high temperatures are seriously hindered by the rapid decay of capacity and insufficient safety [6–8]. For example, the first discharge capacity of NCM811 was 144 $mAhg^{-1}$ at room temperature 25 °C (1 C), and its capacity retention was 82.20% after 200 cycles, while which sharply decline to 74.9% after 100 cycles at 55 °C [9]. It can be clearly seen that nickel-rich materials delivered terrible capacity retention at elevated temperatures. Generally speaking, the decline in lithium-ion battery capacity is mainly due to the degradation of the cathode. On the one hand, high delithiated cathode materials are prone to side reactions with electrolytes, leading to the dissolution of transition metal ions into electrolytes. On the other hand, highly reactive Ni^{4+} ions tend to generate inactive product (NiO) and release oxygen, both of them will cause serious structural instability and cation miscibility of cathode materials [10–15]. In addition, ever-increasing dissolved metal ions migrate and deposit on the negative electrode hinders the migration of lithium ions, it also increases the accumulation of electrolytic decomposition products and affects the electrochemical reaction at the interface between the electrolyte and active cathode material, especially at elevated temperature [16]. These side reactions have a profound impact on the lithiation kinetics at the cathode/electrolyte interface and finally trigger a substantial decline in capacity retention. What's more, with the increasing demands for lithium-ion batteries, the working temperature range of lithium ion battery increases gradually. At present, surface coating is the most direct and effective way to reduce the degradation of the cathode, various coating materials which have been investigated in detail can be divided into following categories: metal oxide, metal fluoride, metal phosphate and

* Corresponding author.
E-mail address: mlydoc@126.com (M. Yuan).

https://doi.org/10.1016/j.jelechem.2019.113197
Received 31 January 2019; Received in revised form 31 May 2019; Accepted 2 June 2019
Available online 04 June 2019
1572-6657/

metal carbonate, such as Al_2O_3 [17], Cr_8O_2 [18], CuO [19], ZrO_2 [20],AlF_3 [21], LiF [22], $LaAlO_3$ [12], $LaPO_4$ [23], $LiAlO_2$ [24], Li_2SiO_3 [25], Li_2CO_3 [26] et al. Although the side reactions during the cycling process have been effectively depressed by these coating materials. However, the initial irreversible capacity loss of various coating materials has not been significantly reduced, and the electrochemical performance under high temperature conditions has not been fully studied.

As compared with other coating materials, the calcium fluoride (CaF_2) possesses more excellent thermodynamically stability for the property of higher bond energy ΔH_f (Ca−F) = 527 kJ/mol compared to ΔH_f (Zr−O) = 159 kJ/mol, ΔH_f (Mg−O) = 363.2 kJ/mol, ΔH_f (Mg−F) = 461.9 kJ/mol, ΔH_f (Si−O) = 460 kJ/mol and ΔH_f (Al−O) = 511 kJ/mol. While to our knowledge, relevant reports on the electrochemical performance of CaF_2 coating NCM811 have not been reported. Herein, to gain further insight into the effects of calcium fluoride coating high nickel materials, a certain amount of calcium fluoride has been coated on NCM811 via wet-chemical method. The structure and morphology of both CaF_2-modified sample and the bare one were discussed in detail. Furthermore, the electrochemical performance of cathode materials with or without CaF_2-modified were systematically investigated and analyzed.

2. Experimental

2.1. Synthesis of CaF_2-modified cathode materials

To prepare CaF_2-modified NCM811, a certain amount of prepared NCM811 (synthesized as previous report [5]) and calcium chloride were dissolved in a solution containing ethanol and distilled water, after ultrasonic dispersion for 20 min, ammonium fluoride solution was slowly dribbled into it under strong magnetic agitation, then kept stirring for 1 h at room temperature. After the reaction, the mixed solution was filtered and washed for three times. Finally, the mixed powder was dried in an oven at 80 °C for 60 min, then baked in a muffle furnace at 500 °C for 5 h to obtain CaF_2-coated material. The coating process is schematically shown in Fig. 1. The samples without and with 1.5 wt%, 3.0 wt%, 4.5 wt% CaF_2-modified were marked as M-NCM0 and M-NCM1.5, M-NCM3, M-NCM4.5 in sequence.

2.2. Structure and morphology

The crystalline structure of all samples was determined by X-ray diffraction (XRD, DX-2700) with Cu-Ka radiation within a 2θ between 3° and 80° at a scan rate of 2°/min. The morphologies and elemental distributions of the samples were conducted on high-resolution transmission electron microscopy (HRTEM, JEOL JEM 2010) and scanning electron microscopy (SEM, JEOL JSM-6360LV) equipped with energy dispersive X-ray spectroscopy (EDS). In addition, surface element composition and oxidation state were elucidated by X-ray photoelectron spectroscopy.

2.3. Electrochemical measurement

Electrochemical performance evaluations were carried out using CR2025 coin-type half cells. The working electrodes were composed of 80 wt% active materials, 10 wt% Super P, and 10 wt% polyvinylidene fluorides (PVDF) dissolved in *N*-methyl-2-pyrrolidinone (NMP). The obtained slurry was then spread uniformly onto an Al foil current collector with a thickness of 50 um and dried at 120 °C in a vacuum oven for 12 h. The diameter of the circular electrode is 12 mm and the mass of active material on it is approximate 1.65 mg/cm^2. The electrolyte was 1 M $LiPF_6$ dissolved in ethylene carbonate (EC) + dimethyl carbonate (DMC) + ethyl methyl carbonate (EMC) (1:1:1 in volume) solution. The CR2025 coin-type half cells were assembled in an argon-filled glove box with pure lithium metal as the counter electrode and Celgard 2400 as the separator, and then aged for 12 h so that the electrolyte can be fully soaked. Galvanostatic charge/discharge tests were measured between 2.7 and 4.3 V using Neware Battery Test System BTS-XWJ-7.4.16S (Neware, China) at different temperatures (25, 55 °C). Besides, the cyclic voltammetry (CV) and electrochemical impedance spectroscopy (EIS) were measured on GAMRY Reference 600 electrochemical workstation, with a scan rate of 0.1 mV/s and a frequency range from 100 kHz to 0.01 Hz, respectively.

3. Results and discussion

3.1. Bulk structure and surface properties of cathode materials

XRD patterns of M-NCM0, M-NCM1.5, M-NCM3 and M-NCM4.5 are

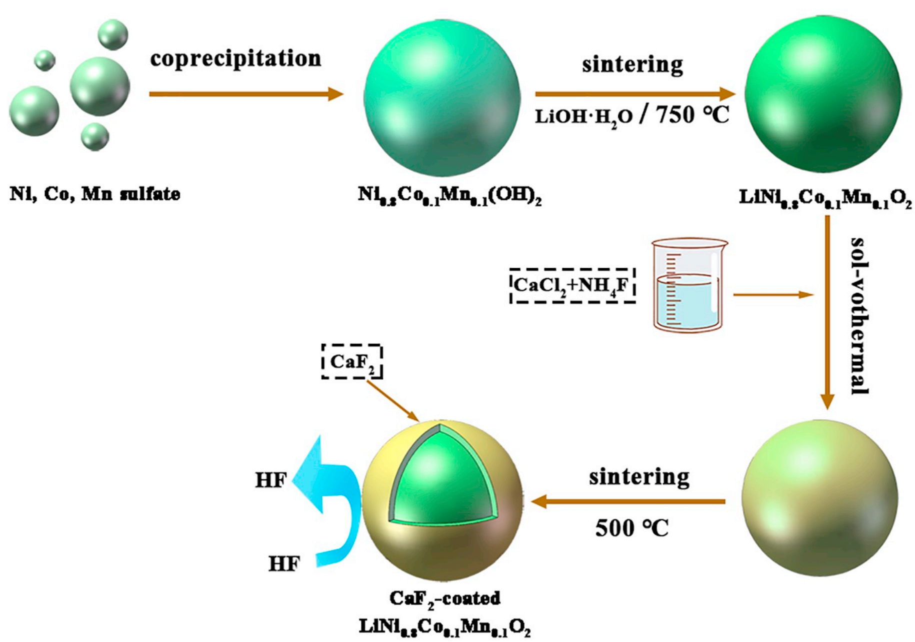

Fig. 1. Schematic of material preparation and CaF_2 coating procedure.

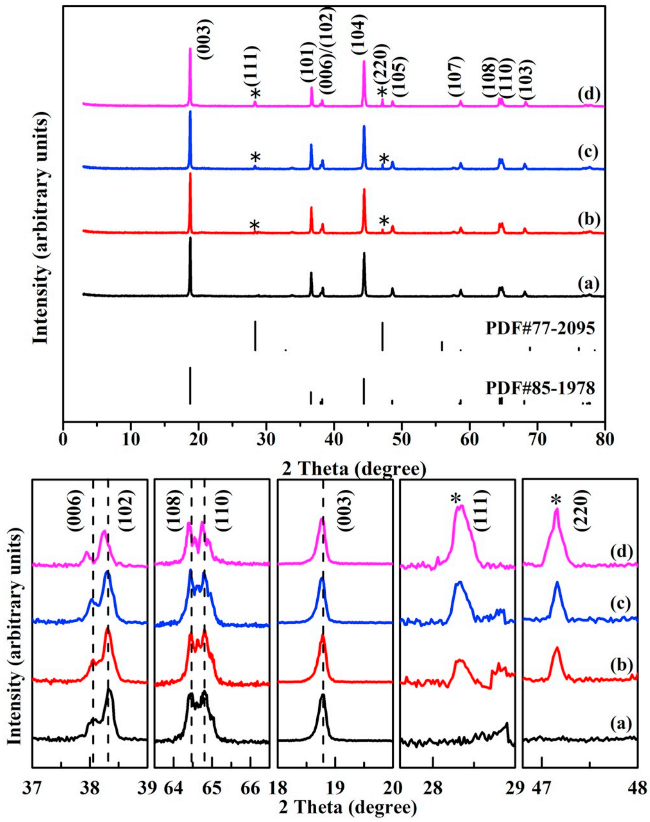

Fig. 2. The XRD patterns of pristine (a), M-NCM1.5 (b), M-NCM3 (c) and M-NCM4.5 (d).

shown in Fig. 2. It is noted in Fig. 2a that all diffraction lines are similar and can be indexed to a rhombohedral α-$NaFeO_2$ structure with a space group of R-3m (PDF#85-1978). The major peaks of all coated samples are generally aligned with the bare one except several extra peaks indexed to CaF_2 phase (PDF#77-2095), these extra peaks are very low and narrow compared to the characteristic peaks of the main phase, which reveals that CaF_2 modification does not change the bulk structure of NCM811. The enlarged XRD patterns in selected 2θ range were shown in Fig. 2b, it can be seen clearly that the characteristic peak of (003) move left slightly and the adjacent peaks (006)/(102) and (108)/(110) are separated distinctly with a little deviation, indicating that both coated and uncoated samples presented a similar well-developed layered structure [27]. Additionally, with the coating amount increases, the diffraction intensity of the main peaks (111) and (220) of CaF_2 enhanced gradually, which initially suggests that CaF_2 was successfully designed in the cathode material.

Table 1 shows the lattice parameters of all samples, the ratio of $I_{(003)}/I_{(104)}$ for different coating amounts was 1.3299 (b), 1.3343 (c), 1.3321 (d) respectively, while the bare one was 1.3274, indicating that CaF_2 coating through wet chemical coating process almost has no adverse effect on the mixing degree of Ni^{+} in the materials [28]. Furthermore, the c/a ratios of the bare and CaF_2-coated samples are both bigger than 4.9, further indicating that the layer structure of all samples possess well crystallinity [29].

To clarify the surface elements and the oxidation states of materials, XPS measurements have been carried out. As shown in Fig. 3(a–c), the binding energies of Ni $2p_{3/2}$, Co $2p_{3/2}$, Mn $2p_{3/2}$ show a similarly value of 854.9/855.1, 779.3/779.4, 642.1/641.9 eV before and after coating, respectively, which correspond to Ni^{2+}, Co^{3+} and Mn^{4+} in the samples, these results reveal that the coating process has little effect on the chemical stability of NCM811 surface elements [23]. However, for M-NCM3, the emerging of Ca $2p_{3/2}$ and F 1s peaks at 347.8 and 684.5 eV in Fig. 3(d–e) implying the existence of Ca^{2+} and F^{-}, suggesting that CaF_2 was formed on the surface of NCM811.

Typical SEM tests were performed on the pristine and different coating materials to get a visualized impression of the materials. As is shown in Fig. 4, all samples present similar monodisperse secondary spherical particles with 8–12 μm in diameter, which consisted of numerous aggregated hexagonal flake particles. Contrary to the smooth and regular M-NCM0 surface, the magnified region shown in Fig. 3(e–h) reveals that the surface morphologies of different coating materials exhibit a rougher and obscured surface morphology, especially at the interface of grains with the increase of coating content. As is clearly seen in Fig. 3h, countless small particles are uniformly attached on the surface of the NCM811 sphere, which preliminary show that CaF_2 layer were successfully coated onto the material surface.

The elementary distribution of 3 wt% calcium fluoride coated sample was illustrated in Fig. 5. It is not difficult to find that the element mappings of Ca and F are homogeneously distributed in the selected region and significantly weaker than that of Ni, Co and Mn. Indicating that the coating thickness is very thin, it is also implied that the coating particles are evenly dispersed and have little effect on the lattice parameters. This is consistent with the XRD and SEM test results.

In order to further evaluate the microscopic structure of pristine and M-NCM3 materials, High-resolution transmission electron microscopy (HRTEM) tests were carried out subsequently. The surface of pristine sample is very smooth without any coating layer, while M-NCM3 particle presented obvious coating layer with a thickness of 5–12 nm, which can be clearly seen at low magnification in Fig. 6a and c, this results strongly support that CaF_2 coating layer has been designed successfully. Moreover, the HRTEM images (Fig. 6b and d) manifest that the lattice fringes of both the bare material and M-NCM3 are approximately 0.47 nm, which is consistent with the (003) plane of high nickel material [30]. It further certificates that the coating process do not affect the internal structure of the material.

Fig. 7a displays the initial charge/discharge performance of the pristine and CaF_2-coated samples at 0.1 C (27.5 $mAhg^{-1}$). It shows that the bare sample has the highest initial charge and discharge specific capacity value of 240.4 and 195.5 $mAhg^{-1}$, while the lowest is M-NCM4.5 of 215.9 and 190.6 $mAhg^{-1}$, which may be related to the different energy storage space of lithium. As shown in Table 1, as the amount of calcium fluoride coating increases, the initial charge and discharge capacity of coated samples decrease slightly. Among them, the initial discharge specific capacity of M-NCM4.5 sample is 190.6 $mAhg^{-1}$ with a coulombic efficiency of 88.28%, while the bare sample is 195.5 $mAhg^{-1}$ with 79.24% retained, it is not difficult to find that all the coated samples kept slightly higher coulombic efficiency than that of the bare material. This may be because CaF_2 coating layer blocks the direct contact between cathode material and electrolyte, thus better protecting the cathode active material and improving its coulombic efficiency. Fig. 7c presents the cycling properties of all samples at 0.1 C between 2.7 and 4.3 V. After 100 cycles, all samples exhibited a slightly decrease in capacity, while compared with the bare NCM811, the surface-modified cathodes maintained a higher discharge capacity. To be specific, with the increasing of calcium fluoride content, the capacity retention rate of pristine, 1.5 wt%, 3 wt%, and 4.5 wt% samples are 95.45, 96.30, 97.72 and 97.80%, respectively. These results preliminarily indicate that CaF_2 coating can provide a higher capacity

Table 1
Lattice parameters of the pristine and CaF_2-modified NCM811 samples.

Samples	a (Å)	c (Å)	c/a	$I_{(003)}/I_{(004)}$
M-NCM0	2.877	14.188	4.9315	1.3274
M-NCM1.5	2.875	14.192	4.9363	1.3299
M-NCM3	2.872	14.198	4.9436	1.3343
M-NCM4.5	2.882	14.205	4.9289	1.3321

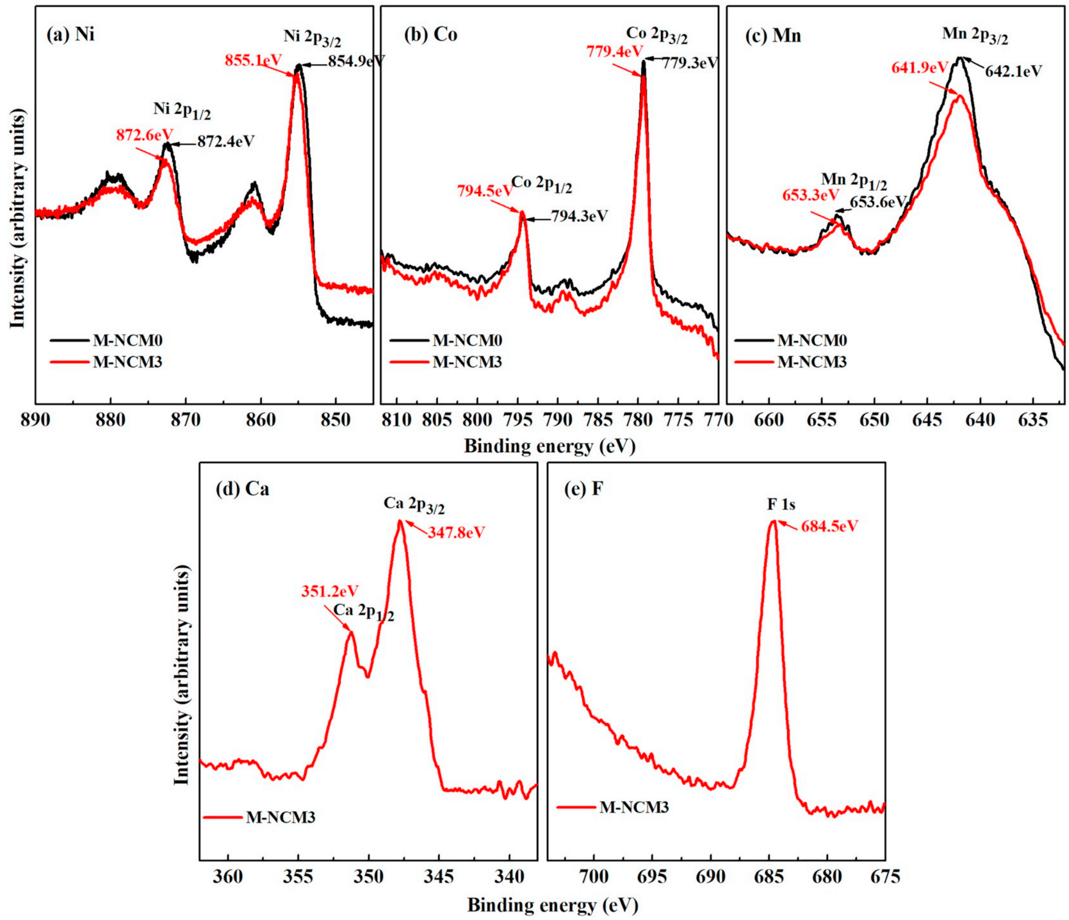

Fig. 3. XPS spectra of the pristine and M-NCM3 samples, (a) Ni 2p, (b)Co 2p, (c) Mn 2p, (d) Ca 2p and (e) F 1s.

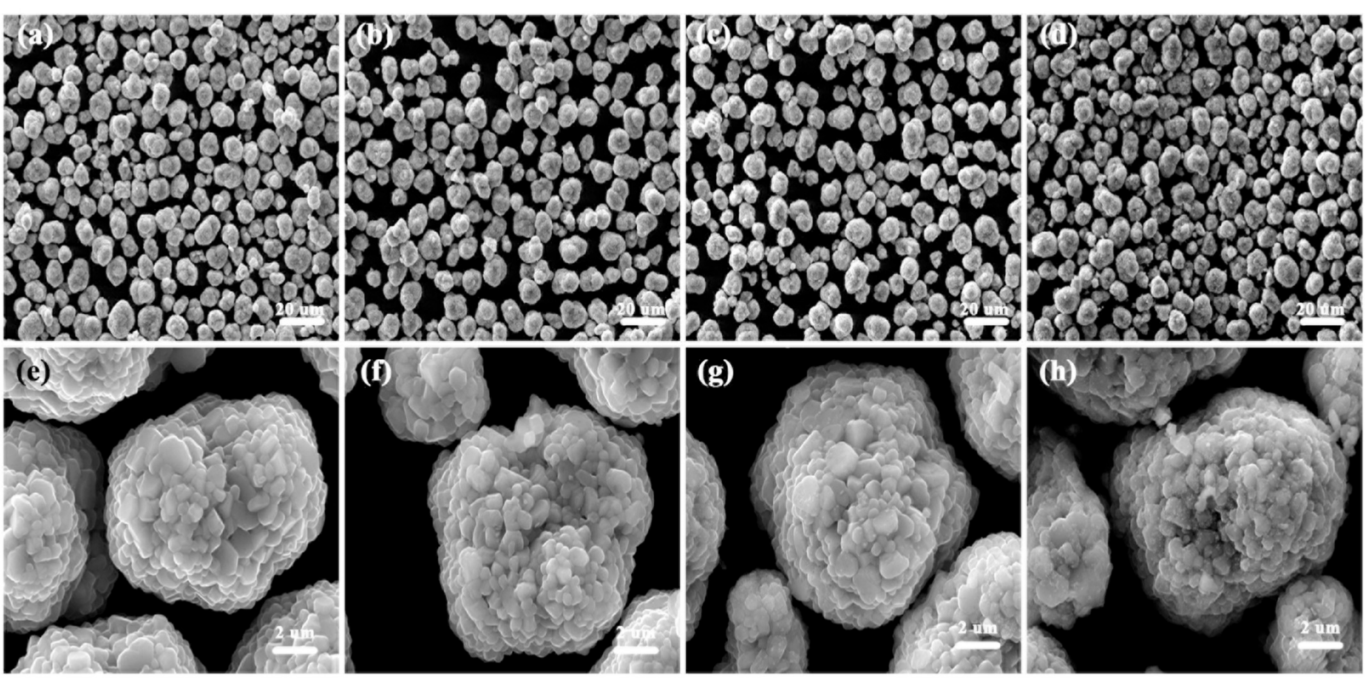

Fig. 4. SEM images of pristine (a, b), M-NCM1.5 (c, d), M-NCM3 (e, f) and M-NCM4.5 (g, h).

retention and better structural stability when cycling at a low current rate.

To investigate the influence of CaF_2 coating on cyclic stability at high rate, cells assembled with bare and surface-modified materials were cycled for 200 times at the rate of 1 C, respectively. As shown in Fig. 8, the capacity of each sample decreased significantly, while it is

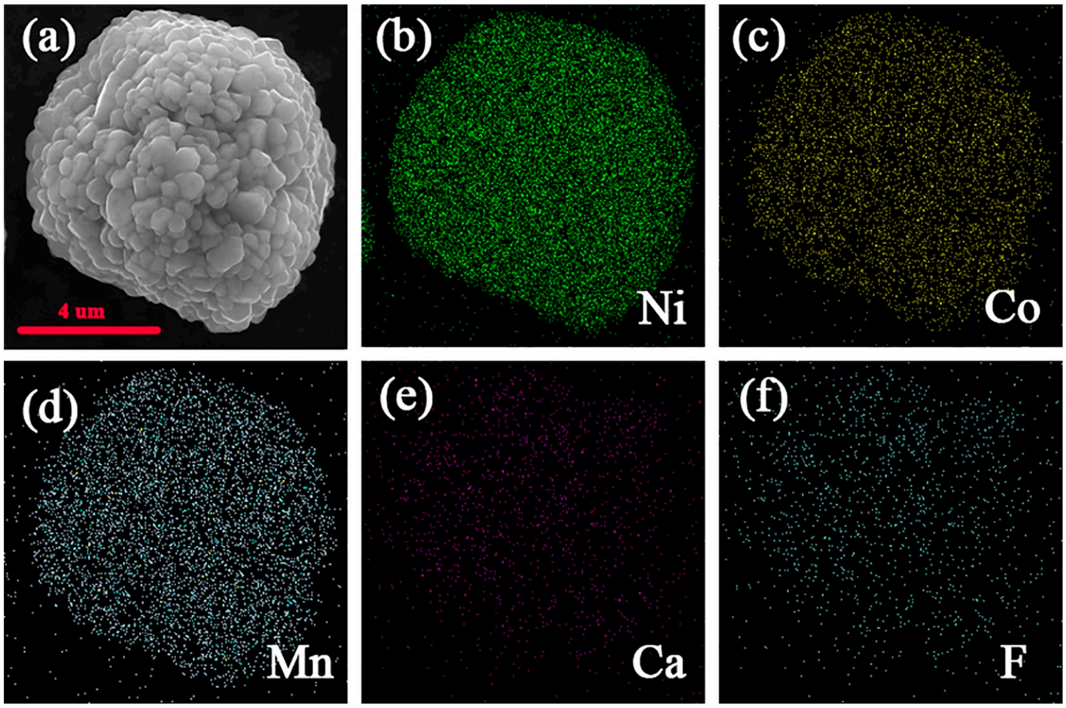

Fig. 5. (a) SEM image of M-NCM3 sample, (b–f) EDS mappings of, Ni, Co, Mn, Ca and F.

worth noticing that the capacity of CaF_2-modified materials declined much more slowly. For example, the capacity retention of bare sample is 79.12% after cycling, fading rapidly from 150.4 to 119.0 $mAhg^{-1}$, while the CaF_2-coated samples reached 82.0%, 85.36%, and 84.04% with the increase of coating amount, respectively (Table 2). The enhancement of rate value may be attributed to the fact that CaF_2 coating effectively reduces the dissolution of the bulk materials in the electrolyte, so as to obtain better material stability when Li^+ intercalation/deintercalation.

Fig. 9a shows the rate capability in the potential range of 2.7–4.3 V

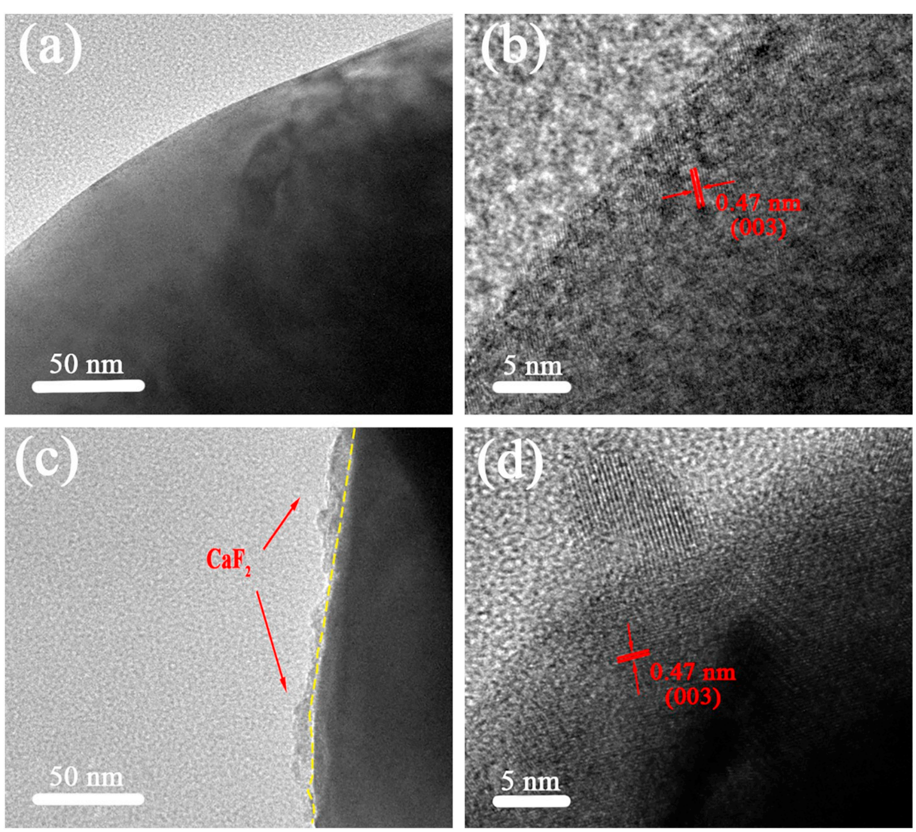

Fig. 6. TEM images of (a) pristine and (c) M-NCM3 samples, HR-TEM images of (b) pristine and (d) M-NCM3 samples.

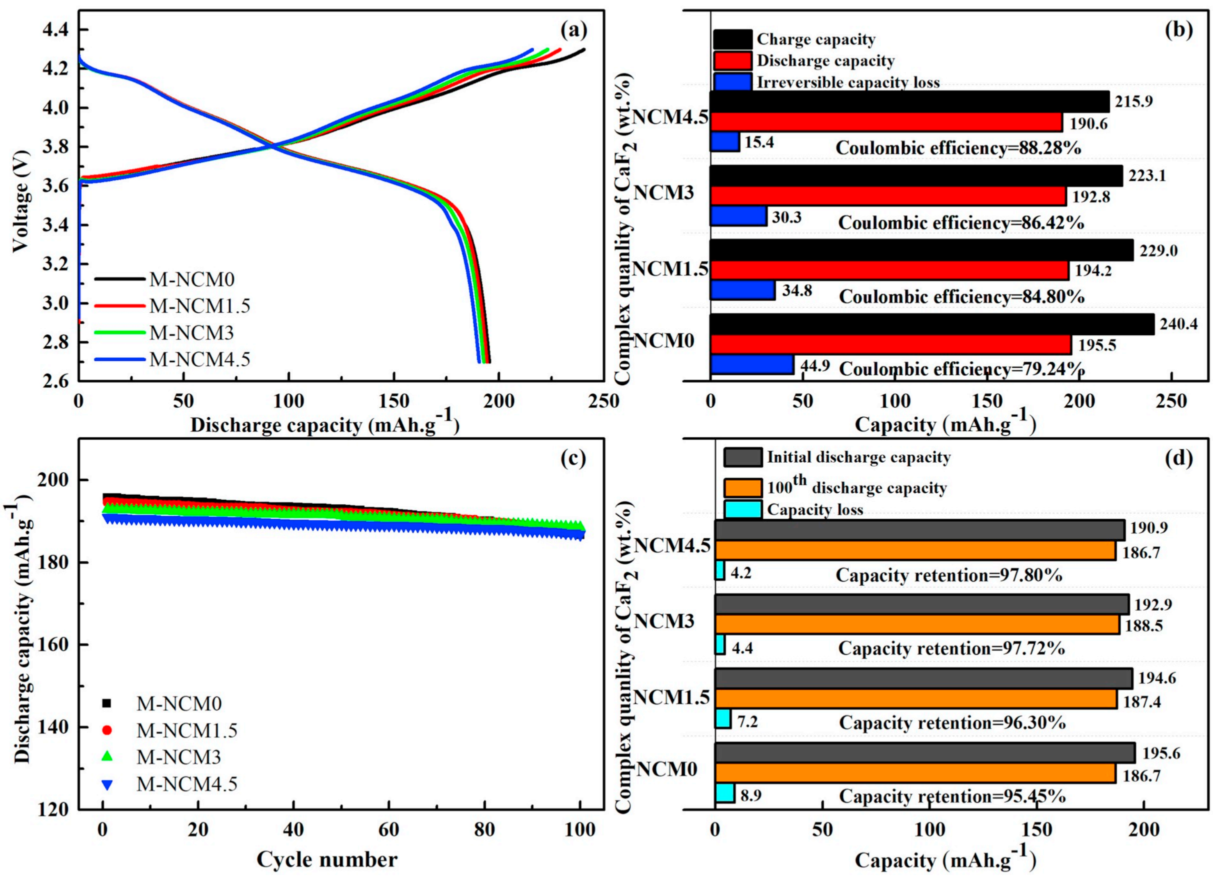

Fig. 7. The initial charge/discharge characteristics of pristine and CaF_2-coated NCM811 samples (a, b), cycling performance at 0.1 C (c, d).

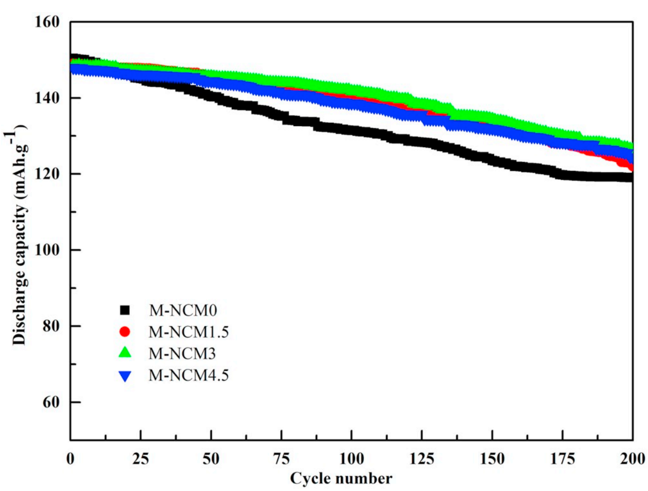

Fig. 8. Cycling capacity at 1 C rate of pristine and CaF_2-coated samples.

Table 2
Electrochemical data of the pristine and CaF_2-modified NCM811 samples at 1 C rate.

Sample	Initial charge capacity ($mAhg^{-1}$)	200th discharge capacity ($mAhg^{-1}$)	Capacity retention (%)
M-NCM0	150.4	119.0	79.12
M-NCM1.5	148.9	122.1	82.00
M-NCM3	148.2	126.5	85.36
M-NCM4.5	147.9	124.3	84.04

at 0.1, 0.2, 0.5, 1, 2, 5 and 0.1 C. Compared to the bare NCM811, it can be clearly seen that the rate capability of CaF_2-coated sample is significantly improved especially at high rate. Among them, M-NCM3 present the best performance, which can deliver 192.6 $mAhg^{-1}$ at the first cycle and 181.7 $mAhg^{-1}$ at the last cycle with capacity retention of 94.34%, while the bare one is only 87.05% from 195.4 $mAhg^{-1}$ to 170.1 $mAhg^{-1}$. In addition, when Li^+ intercalation/deintercalation occurs, it is reported that the valence states of elements in the cathode material especially nickel and manganese, determine the stability of the layered structure and the depth of lithium removal, leading to voltage decay in the cycling process [16]. As shown in Fig. 9b–e, the discharge profiles vs rates are investigated. Obviously, the voltage decay of CaF_2-coated sample is much slower than that of the original one. Combined with the above results, it confirms that the existence of CaF_2 coating layer can effectively improve the cycling performance of NCM811 material.

As we all know, NCM811 is essentially a $LiNiO_2$-based material, while researches show that these materials present a significantly decline in cycling capacity when the environment temperature above 55 °C [4,31]. To characterize the cycling performances of pristine and CaF_2-modified samples at elevated temperature, the assembled cells were placed in 55 °C environment for 50 cycles at the rate of 1 C. As shown in Fig. 10a, cell with NCM-0 presents an initial discharge specific capacity of 150.4 $mAhg^{-1}$ and shows a capacity loss of 40.68% after 50 cycles. In contrast, M-NCM3 exhibits with an initial discharge specific capacity of 149.6 $mAhg^{-1}$ and keep a capacity retention of 79.68% after cycles. Additionally, the coulombic efficiency of pristine and 3% CaF_2-coated samples at 25 and 55 °C is compared in Fig. 10b, it can be seen that there is almost no difference in coulombic efficiency at low temperature, while the coated sample presents a higher and more stable coulombic efficiency at high temperature 55 °C. Therefore, we deduce that that CaF_2 coating layer can improve the cycling

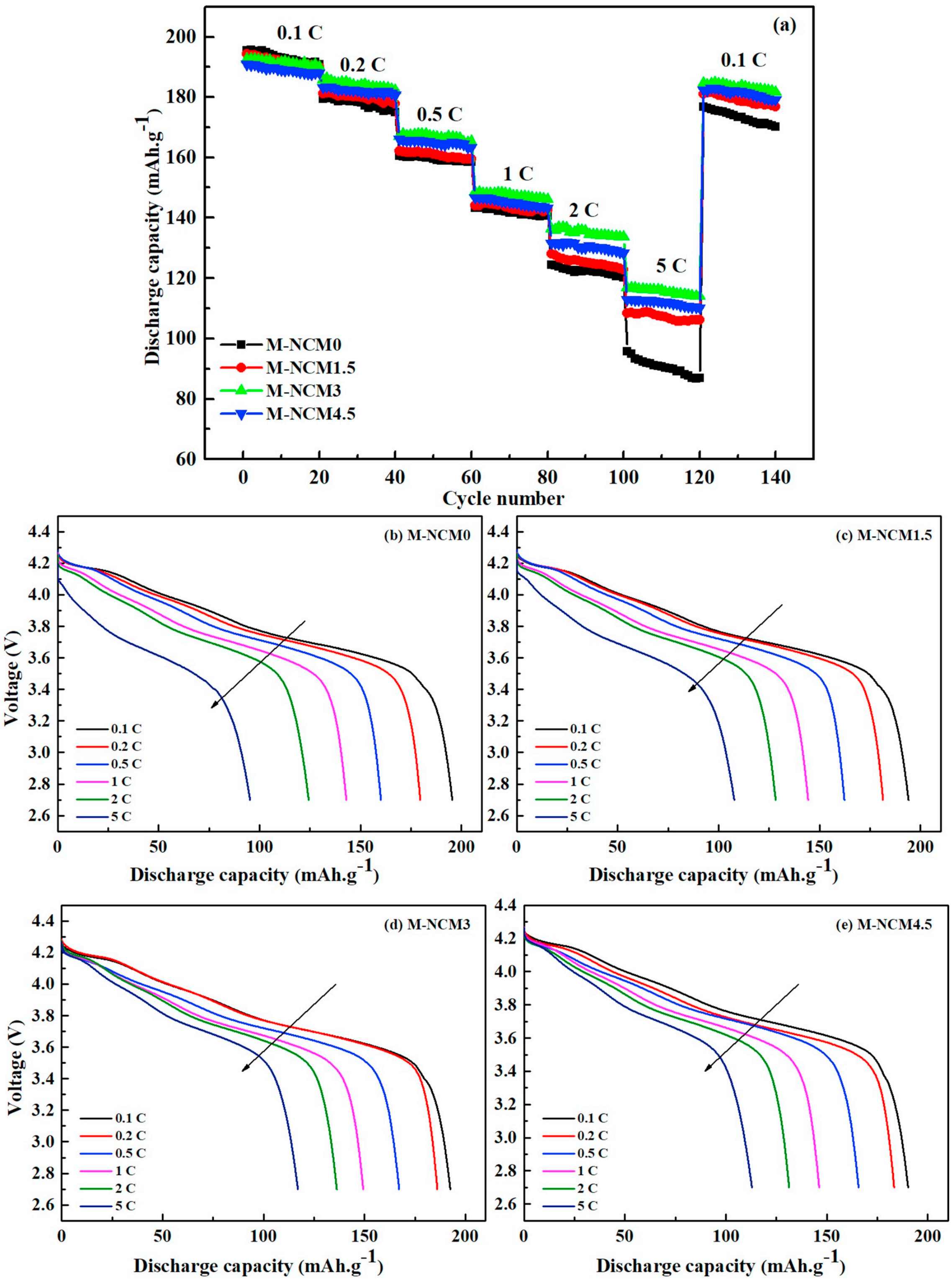

Fig. 9. Rate capability of pristine and CaF_2-coated NCM811 samples (a), discharge profiles vs rates for cells assembled with 0%, 1.5%, 3% and 4.5% CaF_2-coated cathodes (b-e).

performance of NCM811 material at elevated temperature, which is consistence with the results that CaF_2 coating can not only improve the activity and stability of Ni^{4+} ions during the lithiated/delithiated processes, but also inhibit the side reaction between generated HF in electrolyte and material surface even at elevated temperature [32].

The cyclic voltammetry (CV) measurements for the first and 100th cycles were carried out to study the reaction kinetics during the cycling with a scanning rate of 0.1 mVs^{-1}. As shown in Fig. 11, all samples present several peaks at around 3.7 V and 3.8 V, among which the maximum redox peaks correspond to the redox reactions between Ni^{2+}, Ni^{3+} and Ni^{4+} during the charge/discharge process, while another distinct redox peaks are attributed to the transfer between Co^{3+} and Co^{4+} [33]. It is reported that the potential difference (ΔV) between the oxidation peak and the reduction peak is a sign of the reversibility of

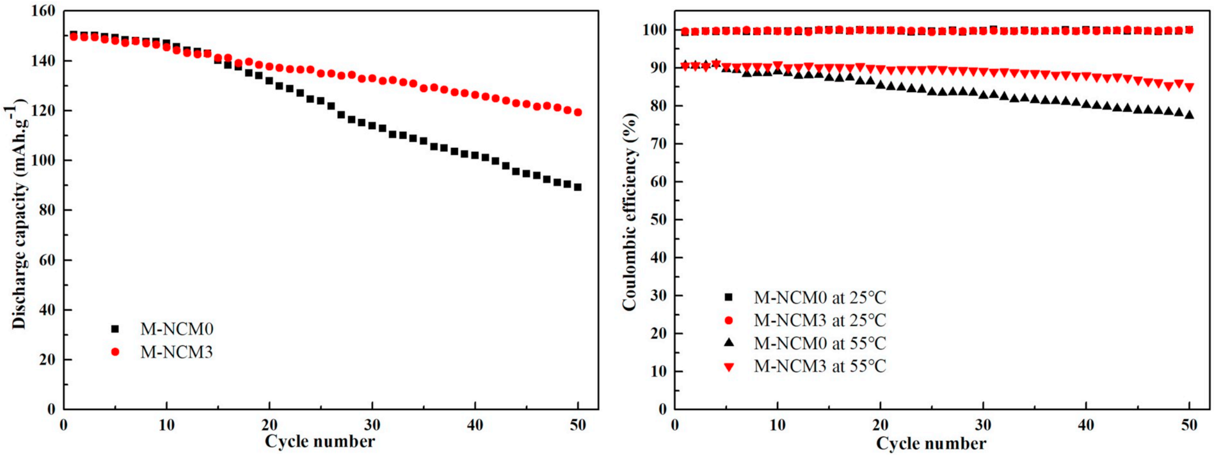

Fig. 10. Cycling capacity of pristine and M-NCM3 samples at 1 C with the potential range from 2.7 to 4.3 V at 55 °C (a), coulombic efficiency of two samples at 25 and 55 °C (b).

the Li^+ extraction/insertion processes, the smaller ΔV means smaller reaction polarization occurred during cycling, which implies a better conduction of Li^+ ions and therefore display an excellent reversibility for electrode material [34]. Among them, M-NCM0 delivers potential difference (ΔV) with 0.1359 V for the first cycle and 0.1049 V after 100 cycles, while the M-NCM3 delivers 0.1306 V and 0.0828 V, respectively. Obviously, the ΔV becomes smaller after 3 wt% CaF_2 coating, it reveals that CaF_2 coating layer can effectively reduce the polarization of the material and enhance the cycling stability of the NCM811 material.

To further reveal the influence of CaF_2 modification, EIS tests were performed for the pristine and various amount of CaF_2 coated samples after the 50th and 100th cycles. The obtained Nyquist plots are given in Fig. 12, it is clearly shows that all of the curves are consisted of an intercept, a semicircle and an oblique line: the resistance intercept in highest frequency region corresponds to ohmic resistance (R_s), the semicircle in medium frequency region is charge transfer resistance (R_{ct}) and a correlated constant phase element CPE_{ct}, the oblique line in the low-frequency region represents to Warburg impedance (W_o) associated with the diffusion impedance of lithium ions in the electrode [23]. Obviously, the impedances of coated sample after 50th cycle was much smaller than that of the unmodified sample, which may be because the protective effect of the coating layer not only makes it easier for lithium ions to diffuse but also facilitates the conduction of electron [35]. What's more, after 100 cycles, it is apparently to find that cells with CaF_2-modified material present a pretty better performance, especially M-NCM3 exhibits with a much lower Rct of 63.2 Ω than the naked sample of 150.3 Ω as shown in Table 3. These results further indicate that calcium fluoride coating layer can effectively protect the active material and enhance the structural stability of NCM811 during the processes of Li^+ intercalation/deintercalation, so as to improve its electrochemical performance.

4. Conclusions

In our research, CaF_2-coated $LiNi_{0.8}Co_{0.1}Mn_{0.1}O_2$ (containing 1.5, 3, and 4.5 wt%) cathode materials were initially designed and prepared via a simple wet chemical method. The structural characteristics and electrochemical performance of materials before and after coating were systematically investigated. The morphological studies show that a CaF_2 layer with a thickness of 5–12 nm was uniformly distributed on the surface of microspheres without obvious structural or morphological changes. Additionally, electrochemical results indicate that the rate capability and cycling stability are significantly improved after coating, especially M-NCM3, which exhibits better initial discharge specific capacity of 192.8 mAhg^{-1}, corresponding to 86.42% coulombic efficiency. Furthermore, CV and EIS results reveal that M-NCM3 exhibits a smaller potential difference (ΔV) and impedance after cycles, further indicating that calcium fluoride coating has a positive effect on the structural stability of NCM811 material during the cycle. The main reason is that the coating can not only effectively alleviate the dissolution of the bulk materials in electrolyte but also improve the stability of NCM811 material during Li^+ intercalation/deintercalation. The approach for structural stability and electrochemical performance

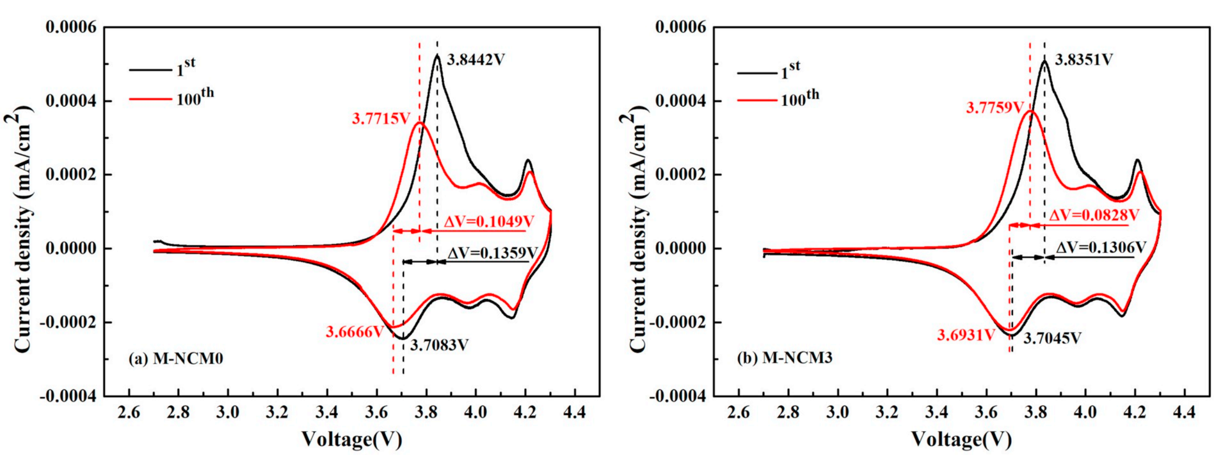

Fig. 11. Cyclic voltammograms curves of (a) pristine, (b) M-NCM3 samples with a scan rate of 0.1 mVs^{-1}.

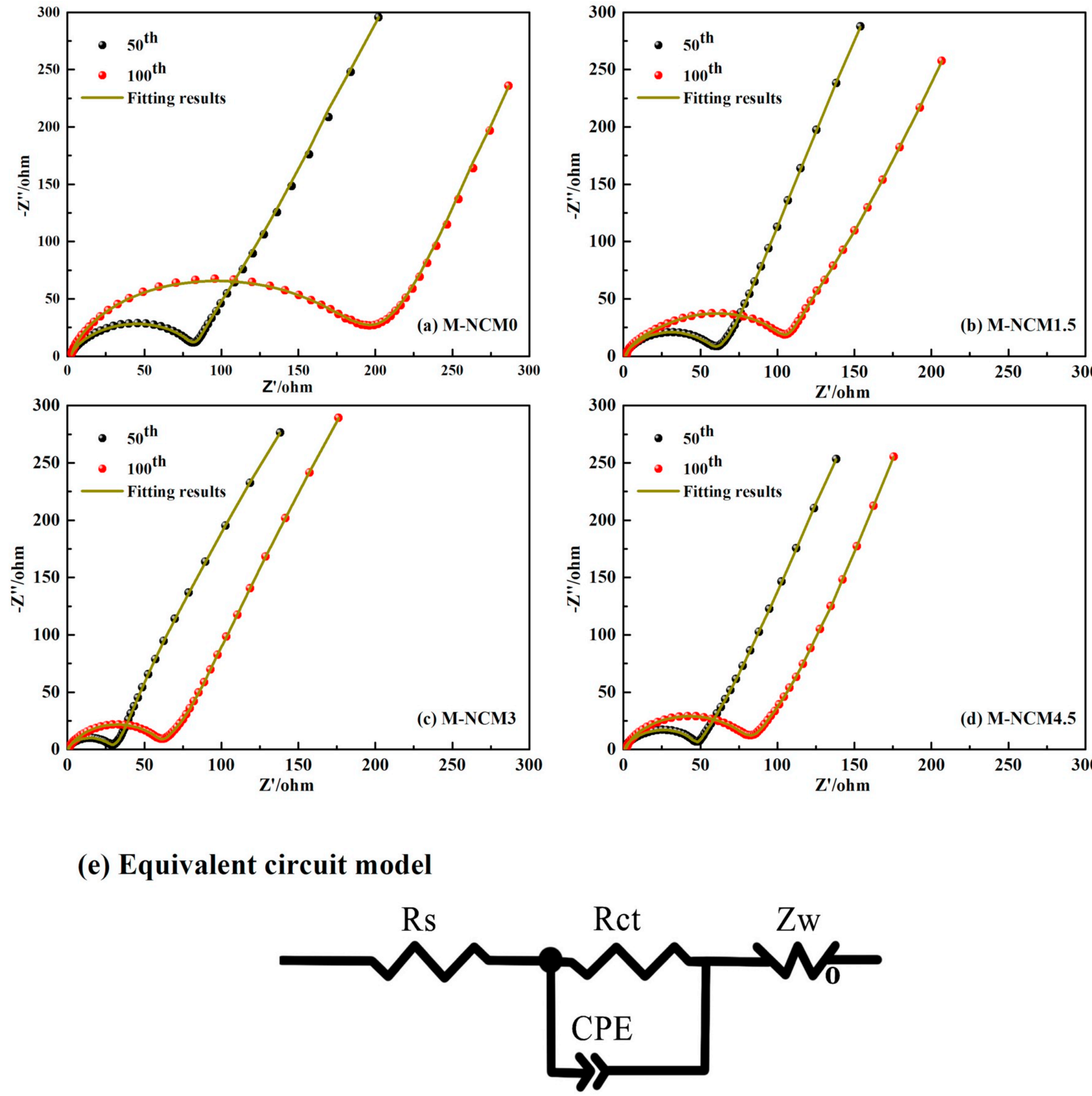

Fig. 12. EIS Nyquist plots of pristine (a) and 1.5, 3, and 4.5 wt% CaF_2-coated samples (b–d), (e) the equivalent circuit for EIS results fitting.

Table 3
Charge-transfer resistance (Rct, Ω) of pristine and 1.5, 3.0 and 4.5 wt% CaF_2-modified samples at various cycles.

Samples	The 50th cycle	The 100th cycle
M-NCM0	82.3	150.3
M-NCM1.5	59.7	104.6
M-NCM3	29.1	63.2
M-NCM4.5	48.3	83.8

enhancement of $LiNi_{0.8}Co_{0.1}Mn_{0.1}O_2$ presented in the paper provide a new idea for surface modification, and this effective composition strategy can be extended to other lithium battery cathode material modification.

Acknowledgement

This work was supported by the Major Science and Technology Research of Guangxi Department of Funded Projects (Grant No. 1114022-15).

Appendix A. Supplementary data

Supplementary data to this article can be found online at https://doi.org/10.1016/j.jelechem.2019.113197.

References

[1] M. Armand, J.M. Tarascon, Building better batteries, Nature 451 (2008) 652–657.
[2] P.G. Bruce, B. Scrosati, J.M. Tarascon, Nanomaterials for rechargeable lithium batteries, Angewandte Chemie-International Edition 47 (2008) 2930–2946.
[3] S. Chen, T. He, Y. Su, Y. Lu, L. Bao, L. Chen, Q. Zhang, J. Wang, R. Chen, F. Wu, Ni-rich $LiNi_{0.8}Co_{0.1}Mn_{0.1}O_2$ oxide coated by dual-conductive layers as high performance cathode material for lithium-ion batteries, ACS Appl. Mater. Interfaces 9 (2017) 29732–29743.
[4] A.M. Andersson, D.P. Abraham, R. Haasch, S. MacLaren, J. Liu, K. Amine, Surface characterization of electrodes from high power lithium-ion batteries, J. Electrochem. Soc. 149 (2002) A1358.
[5] S. Dai, M. Yuan, L. Wang, L. Luo, Q. Chen, T. Xie, Y. Li, Y. Yang, Ultrathin-Y_2O_3-coated $LiNi_{0.8}Co_{0.1}Mn_{0.1}O_2$ as cathode materials for Li-ion batteries: synthesis, performance and reversibility, Ceram. Int. 45 (2019) 674–680.
[6] M.-T.F. Rodrigues, G. Babu, H. Gullapalli, K. Kalaga, F.N. Sayed, K. Kato, J. Joyner, P.M. Ajayan, A materials perspective on Li-ion batteries at extreme temperatures, Nat. Energy 2 (2017) 17108.
[7] J. Xia, L. Ma, K.J. Nelson, M. Nie, Z. Lu, J.R. Dahn, A study of Li-ion cells operated to 4.5 V and at 55 °C, J. Electrochem. Soc. 163 (2016) A2399–A2406.
[8] Y. Xi, Y. Liu, D. Zhang, S. Jin, R. Zhang, M. Jin, Comparative study of the

electrochemical performance of $LiNi_{0.5}Co_{0.2}Mn_{0.3}O_2$ and $LiNi_{0.8}Co_{0.1}Mn_{0.1}O_2$ cathode materials for lithium ion batteries, Solid State Ionics 327 (2018) 27–31.
[9] Q. Li, R. Dang, M. Chen, Y. Lee, Z. Hu, X. Xiao, Synthesis method for long cycle life lithium-ion cathode material: nickel-rich core-shell $LiNi_{0.8}Co_{0.1}Mn_{0.1}O_2$, ACS Appl. Mater. Interfaces 10 (2018) 17850–17860.
[10] Z. Chen, J. Wang, J. Huang, T. Fu, G. Sun, S. Lai, R. Zhou, K. Li, J. Zhao, The high-temperature and high-humidity storage behaviors and electrochemical degradation mechanism of $LiNi_{0.6}Co_{0.2}Mn_{0.2}O_2$ cathode material for lithium ion batteries, J. Power Sources 363 (2017) 168–176.
[11] W. Cho, S.-M. Kim, K.-W. Lee, J.H. Song, Y.N. Jo, T. Yim, H. Kim, J.-S. Kim, Y.-J. Kim, Investigation of new manganese orthophosphate $Mn_3(PO_4)_2$ coating for nickel-rich $LiNi_{0.6}Co_{0.2}Mn_{0.2}O_2$ cathode and improvement of its thermal properties, Electrochim. Acta 198 (2016) 77–83.
[12] Y.-C. Li, W.-M. Zhao, W. Xiang, Z.-G. Wu, Z.-G. Yang, C.-L. Xu, Y.-D. Xu, E.-H. Wang, C.-J. Wu, X.-D. Guo, Promoting the electrochemical performance of $LiNi_{0.8}Co_{0.1}Mn_{0.1}O_2$ cathode via $LaAlO_3$ coating, J. Alloys Compd. 766 (2018) 546–555.
[13] Y.-D. Xu, W. Xiang, Z.-G. Wu, C.-L. Xu, Y.-C. Li, X.-D. Guo, G.-P. Lv, X. Peng, B.-H. Zhong, Improving cycling performance and rate capability of Ni-rich $LiNi_{0.8}Co_{0.1}Mn_{0.1}O_2$ cathode materials by $Li_4Ti_5O_{12}$ coating, Electrochim. Acta 268 (2018) 358–365.
[14] D. Wang, X. Li, Z. Wang, H. Guo, Y. Xu, Y. Fan, J. Ru, Role of zirconium dopant on the structure and high voltage electrochemical performances of $LiNi_{0.5}Co_{0.2}Mn_{0.3}O_2$ cathode materials for lithium ion batteries, Electrochim. Acta 188 (2016) 48–56.
[15] Y.X. Wang, K.H. Shang, W. He, X.P. Ai, Y.L. Cao, H.X. Yang, Magnesium-doped $Li_{1.2}[Co_{0.13}Ni_{0.13}Mn_{0.54}]O_2$ for lithium-ion battery cathode with enhanced cycling stability and rate capability, ACS Appl. Mater. Interfaces 7 (2015) 13014–13021.
[16] S. Liu, J. Su, J. Zhao, X. Chen, C. Zhang, T. Huang, J. Wu, A. Yu, Unraveling the capacity fading mechanisms of $LiNi_{0.6}Co_{0.2}Mn_{0.2}O_2$ at elevated temperatures, J. Power Sources 393 (2018) 92–98.
[17] Z. Cao, Y. Li, M. Shi, G. Zhu, R. Zhang, X. Li, H. Yue, S. Yang, Improvement of the cycling performance and thermal stability of lithium-ion batteries by coating cathode materials with Al_2O_3 nano layer, J. Electrochem. Soc. 164 (2017) A475–A481.
[18] J. Yang, Z. Yu, B. Yang, H. Liu, J. Hao, T. Yu, K. Chen, Electrochemical characterization of Cr_8O_{21} modified $LiNi_{0.5}Co_{0.2}Mn_{0.3}O_2$ cathode material, Electrochim. Acta 266 (2018) 342–347.
[19] T. Liu, S.-X. Zhao, K. Wang, C.-W. Nan, CuO-coated $Li[Ni_{0.5}Co_{0.2}Mn_{0.3}]O_2$ cathode material with improved cycling performance at high rates, Electrochim. Acta 85 (2012) 605–611.
[20] T. Tao, C. Chen, Y. Yao, B. Liang, S. Lu, Y. Chen, Enhanced electrochemical performance of ZrO_2 modified $LiNi_{0.6}Co_{0.2}Mn_{0.2}O_2$ cathode material for lithium ion batteries, Ceram. Int. 43 (2017) 15173–15178.
[21] D. Chen, W. Tu, M. Chen, P. Hong, X. Zhong, Y. Zhu, Q. Yu, W. Li, Synthesis and performances of Li-rich@AlF_3@graphene as cathode of lithium ion battery, Electrochim. Acta 193 (2016) 45–53.
[22] X. Xiong, Z. Wang, X. Yin, H. Guo, X. Li, A modified LiF coating process to enhance the electrochemical performance characteristics of $LiNi_{0.8}Co_{0.1}Mn_{0.1}O_2$ cathode materials, Mater. Lett. 110 (2013) 4–9.
[23] H. Tong, P. Dong, J. Zhang, J. Zheng, W. Yu, K. Wei, B. Zhang, Z. Liu, D. Chu, Cathode material $LiNi_{0.8}Co_{0.1}Mn_{0.1}O_2/LaPO_4$ with high electrochemical performance for lithium-ion batteries, J. Alloys Compd. 764 (2018) 44–50.
[24] W. Liu, X. Li, D. Xiong, Y. Hao, J. Li, H. Kou, B. Yan, D. Li, S. Lu, A. Koo, K. Adair, X. Sun, Significantly improving cycling performance of cathodes in lithium ion batteries: the effect of Al_2O_3 and $LiAlO_2$ coatings on $LiNi_{0.6}Co_{0.2}Mn_{0.2}O_2$, Nano Energy 44 (2018) 111–120.
[25] E. Zhao, M. Chen, Z. Hu, D. Chen, L. Yang, X. Xiao, Improved cycle stability of high-capacity Ni-rich $LiNi_{0.8}Co_{0.1}Mn_{0.1}O_2$ at high cut-off voltage by Li_2SiO_3 coating, J. Power Sources 343 (2017) 345–353.
[26] G.V. Zhuang, G. Chen, J. Shim, X. Song, P.N. Ross, T.J. Richardson, Li_2CO_3 in $LiNi_{0.8}Co_{0.15}Al_{0.05}O_2$ cathodes and its effects on capacity and power, J. Power Sources 134 (2004) 293–297.
[27] Q. Li, G. Li, C. Fu, D. Luo, J. Fan, L. Li, K+-doped $Li_{1.2}Mn_{0.54}Co_{0.13}Ni_{0.13}O_2$: a novel cathode material with an enhanced cycling stability for lithium-ion batteries, ACS Appl. Mater. Interfaces 6 (2014) 10330–10341.
[28] Q. Chen, L. Luo, L. Wang, T. Xie, S. Dai, Y. Yang, Y. Li, M. Yuan, Enhanced electrochemical properties of Y_2O_3-coated-(lithium-manganese)-rich layered oxides as cathode materials for use in lithium-ion batteries, J. Alloys Compd. 735 (2018) 1778–1786.
[29] M. Zhang, H. Zhao, M. Tan, J. Liu, Y. Hu, S. Liu, X. Shu, H. Li, Q. Ran, J. Cai, X. Liu, Yttrium modified Ni-rich $LiNi_{0.8}Co_{0.1}Mn_{0.1}O_2$ with enhanced electrochemical performance as high energy density cathode material at 4.5 V high voltage, J. Alloys Compd. 774 (2019) 82–92.
[30] S. Liu, X. Chen, J. Zhao, J. Su, C. Zhang, T. Huang, J. Wu, A. Yu, Uncovering the role of Nb modification in improving the structure stability and electrochemical performance of $LiNi_{0.6}Co_{0.2}Mn_{0.2}O_2$ cathode charged at higher voltage of 4.5 V, J. Power Sources 374 (2018) 149–157.
[31] S. Chen, T. He, Y. Su, Y. Lu, L. Bao, L. Chen, Q. Zhang, J. Wang, R. Chen, F. Wu, Ni-rich $LiNi_{0.8}Co_{0.1}Mn_{0.1}O_2$ oxide coated by dual-conductive layers as high performance cathode material for lithium-ion batteries, ACS Appl. Mater. Interfaces 9 (2017) 29732–29743.
[32] W. Wang, Z. Yin, Z. Wang, X. Li, H. Guo, Effect of heat-treatment on electrochemical performance of Li_3VO_4-coated $LiNi_{1/3}Co_{1/3}Mn_{1/3}O_2$ cathode materials, Mater. Lett. 160 (2015) 298–301.
[33] H. Kim, M.G. Kim, H.Y. Jeong, H. Nam, J. Cho, A new coating method for alleviating surface degradation of $LiNi_{0.6}Co_{0.2}Mn_{0.2}O_2$ cathode material: nanoscale surface treatment of primary particles, Nano Lett. 15 (2015) 2111–2119.
[34] D. Wang, X. Li, Z. Wang, H. Guo, Z. Huang, L. Kong, J. Ru, Improved high voltage electrochemical performance of Li_2ZrO_3-coated $LiNi_{0.5}Co_{0.2}Mn_{0.3}O_2$ cathode material, J. Alloys Compd. 647 (2015) 612–619.
[35] F. Wu, J. Tian, Y. Su, Y. Guan, Y. Jin, Z. Wang, T. He, L. Bao, S. Chen, Lithium-active molybdenum trioxide coated $LiNi_{0.5}Co_{0.2}Mn_{0.3}O_2$ cathode material with enhanced electrochemical properties for lithium-ion batteries, J. Power Sources 269 (2014) 747–754.